

# Microwave Assisted Vacuum Drying Processing: Magnetron vs Solid State. Case Study: Apple Drying

C. Bianchi<sup>1\*</sup>, R. Schmid<sup>1</sup>, D. Frick<sup>1</sup>, S. Kurtz<sup>2</sup>

1. Research and Development Department, Gigatherm AG, Flawil (SG), Switzerland

2. Technology Centre, Food Application, Gigatherm AG Food, Flawil (SG), Switzerland

\*Corresponding author: [bianchi@gigatherm.ch](mailto:bianchi@gigatherm.ch)

## Abstract:

The purpose of the current study is to simulate with COMSOL<sup>®</sup> software the physical behavior in terms of electromagnetic distribution, temperature and moisture content during a food vacuum drying process, comparing a classical magnetron source, a one port solid-state source and a two ports solid-state source. The model is characterized by a vacuum chamber, a turntable, a waveguide (or two in the case of the 2 ports system) and food product. The simulated physics includes the evaporation and diffusion of water which is contained in the food, rotational movement of the turntable, electromagnetic changes of frequency and phase-shift at the ports. The modules that have been used to implement the process are RF Module, CAD import Module, and, other physics interfaces like PDE interface (to implement rotation and evaporation/diffusion) and the Heat Transfer Module. The results show that power is mostly absorbed by the parts of food which are closer to the rim, and thus, drying is faster at the border. By increasing the number of degrees of freedom in terms of generated electromagnetic patterns, it is possible to facilitate the dissipation of heat even in central zone of the processed food.

**Keywords:** microwave heating, vacuum drying, food processing.

## Introduction

The purpose of the current work is to compare different design options for vacuum drying processing with the assistance of microwave radiation. The goal of the process is to remove water content in food products for preservation. Vacuum drying yields inhibition of microbial growth, extended shelf-life, and less weight for transportation. External heat is provided to shortening the process by providing the necessary energy for the phase-change transformation. The treatment must be run gently to avoid damaging of the food products, and thus, the temperature of the heat source cannot be raised, and consequently limiting the process velocity. By assisting the process with microwaves, it is possible to convert energy directly in the material to be dried with a very high absorption selectivity [1]. The process effectivity increases, and the overall time duration can be reduced. Converted electromagnetic power is deposited only in the food and it is not wasted in the surrounding environment. Energy transfer rate is not related to temperature gradients and so the limit of the process velocity is less critical. On the other hand, there are some drawbacks that can occur when using microwave radiation if proper control of the system and/or suitable design are not provided. From a physical point of view, microwaves can propagate and resonate in an enclosed metallic cavity forming a complex electric field pattern which is determined by the geometry of the system, the dielectric

properties of materials (in terms of polarization and absorption) and the radiant source. Peaks and minima of the electric field can induce non-uniform heating patterns, and therefore, can induce also lower food quality. In order to avoid these issues, specific design choices must be taken by adopting numerical computation and optimization to improve the system performances. In the current work, we present a comparison of the heating performances which are related to different microwave technologies: a) magnetron technology, b) 1 channel solid-state technology, c) 2 channels solid-state technology. In the first case, the frequency is fixed and cannot be controlled externally. In the second case, the frequency can be changed in a range belonging to the ISM band. In the third case, the frequency and the phase shift between channels can be controlled [2]. In all the cases, a mechanical rotation of the turntable is included (mechanical steerer). The load is made by apple cubes which are placed in a circular plate. Electric field configurations, power density, temperature and moisture content are assessed over the process duration.

## Theory

The underpinning physics of the process is characterized by the following elements:

- Microwave radiation propagates from the source(s) into the dielectric materials which are present within the chamber
- Electromagnetic power is converted to heat because of polarization and molecular friction due to the attempt of water molecules to get aligned with the oscillating electric field lines at high frequencies (more than 2 billion times per second).
- Heat propagates in the food product and it is generated by the external electromagnetic source, and it is sunk to provide the evaporation energy for the phase change transformation (latent heat).
- Evaporation occurs as a combination of low pressure in the chamber and the external energy. Moisture diffuses in the load and gets removed by liquid due to gas transformation.
- The food is contained in a circular turntable which is rotating around a central axis located in the middle of the plate.

Regarding microwave radiation for the presented cases, magnetron sources can generate microwave radiation with a frequency that is determined by the geometrical shape of the resonant lobes of the magnetron, and by the operative working conditions of the system following the Rieke diagram. Therefore, the frequency is fixed in such a way that it is included in the ISM band and it cannot be changed by the user. The one channel solid-state source is characterized by an internal oscillator that generates electronically the signal at the frequency that is desired and then, by using new generation high power amplifiers, it is possible to raise the signal up to hundreds of Watt. The two channels solid-state source is characterized by the same characteristics of the one channel SSD, but with the added possibility to control the phase shift between the different channels [3]. In this way, it is possible [4] to exploit the constructive and destructive interference of the field patterns over space.

## Implemented governing equations

### Electromagnetics

Maxwell's equations in the phasorial form (Steinmetz transformation) can be expressed as follows:

$$\nabla \times \mathbf{E} = -j\omega\mathbf{B} \quad (1)$$

$$\nabla \times \mathbf{H} = \mathbf{J} + j\omega\mathbf{D} \quad (2)$$

and including the material constitutive laws:

$$\mathbf{J} = \sigma\mathbf{E} \quad (3)$$

$$\mathbf{B} = \mu\mathbf{H} \quad (4)$$

$$\mathbf{D} = \epsilon\mathbf{E} \quad (5)$$

the complex permittivity is:

$$\dot{\epsilon} = \epsilon - \frac{j\sigma}{\omega} \quad (6)$$

We can express the complex permittivity in relative terms dividing by  $\epsilon_0$

$$\epsilon = \epsilon_r - \frac{j\sigma}{\omega\epsilon_0} = \epsilon' - j\epsilon'' \quad (7)$$

The propagation constant in free space is defined as follows:

$$k_0 = \omega\sqrt{\mu_0\epsilon_0} \quad (8)$$

Applying the curl to eq.1 and substituting the above terms, we can derive a partial differential equation for the electric field:

$$\nabla \times \mu^{-1}\nabla \times \mathbf{E} - k_0\epsilon_r\mathbf{E} = 0 \quad (9)$$

Static Power Dissipation (SPD) in the load is:

$$\text{spd}(x, y, z) = 2\pi f\epsilon_0\epsilon_r''|\mathbf{E}(x, y, z)|^2 \quad (10)$$

### Rotation and electric field reconfiguration

Given the static power density, it is possible to derive the Instantaneous Power Density (IPD) over time by considering the angular rotation of the turntable:

$$\text{ipd}(x, y, z, t) = \sum_i \text{spd}_i(x + X_r, y, z + Z_r - Z_g) \cdot pw_i(\text{prob}(t)) \quad (11)$$

Where the rotation space variables are:

$$X_r = (X_g - X_0) \cdot \cos(2\pi f_{rot}t) - (Z_g - Z_0) \cdot \sin(2\pi f_{rot}t) + X_0 \quad (12)$$

$$Z_r = (X_g - X_0) \cdot \sin(2\pi f_{rot}t) - (Z_g - Z_0) \cdot \cos(2\pi f_{rot}t) + Z_0 \quad (13)$$

Where  $i$  spans from 1 to  $k$  (number of the possible configurations of the electric field generated by each specific technology). For a magnetron source  $k = 1$ . For the one channel solid-state source, the possible configurations depend on the frequency sweep  $(f_1, \dots, f_k)$ . For the two channels solid-state source, the possible configurations are related to the combined frequency and phase-shift sweeps:  $((f_1, \Delta\phi_1)_1, \dots, (f_a, \Delta\phi_b)_k)$ , where  $k = ab$ . The rectangular pulse functions  $pw_i: \mathbb{R} \in [0,1] \rightarrow \mathbb{N} \in (0,1)$  are defined as follows:

$$\begin{cases} pw_i(s) = 0 & 0 < s < \frac{i-1}{k} \\ pw_i(s) = 1 & \frac{i-1}{k} < s < \frac{i}{k} \\ pw_i(s) = 0 & 1 > s > \frac{i}{k} \end{cases} \quad (14)$$

The probability function values range from 0 to 1 following a uniform distribution. Values are picked randomly over time to select one of the possible electromagnetic configurations that change over time. The Average Power Density (APD) is computed as the integration of IPD over one complete rotation:

$$apd(x, y, z) = f_{rot} \int_{f_{rot}}^1 ipd(x, y, z, t) dt \quad (15)$$

This function is the actual term that can be elaborated by the heat and moisture transfer physics.

### Heat and moisture transfer

The basic equation of heat transfer is the energy equation:

$$\rho c_p \frac{\partial T}{\partial t} + \rho c_p \cdot \nabla T + \nabla \cdot \mathbf{q} = apd(x, y, z) - \dot{m} \Delta H \quad (16)$$

The right side of the equation shows that the overall absorbed power depends on the electromagnetic power, and, on the lost energy rate due to moisture evaporation. The drying process is driven by the moisture transfer equation:

$$\frac{\partial \theta_l}{\partial t} + \nabla \cdot (-c \nabla \theta_l) = -\frac{\dot{m}}{\rho_l} \quad (17)$$

$$\dot{m} = k_{vap} \rho_l \left( \frac{P_{sat}(T) - P_{ch}}{P_{ch}} \right) \quad (18)$$

Eq.18 is valid only if  $P_{sat} \geq P_{ch}$  and  $\theta_l > \theta_{res}$ , otherwise this term goes to 0.  $k_{vap}$  depends on the specific conditions of food processing. The material properties are strongly affected by the moisture content and they are computed as the weighted average of the mixture liquid ( $l$ ), solid ( $s$ ) and gas ( $g$ ) [4, 5]:

$$\rho_{eff} = \theta_l \rho_l + \theta_s \rho_s + \theta_g \rho_g \quad (19)$$

$$c_{p, eff} = (\theta_l \rho_l c_{p, l} + \theta_s \rho_s c_{p, s} + \theta_g \rho_g c_{p, g}) / \rho_{eff} \quad (20)$$

The saturation pressure curve is available in scientific literature [6].  $k_{vap}$  and  $\lambda_{eff}$  are functions of the food product and should be experimentally

determined or found in literature [7]. Complex electric permittivity can be strongly affected by the moisture content and temperature as presented in Figure 1.

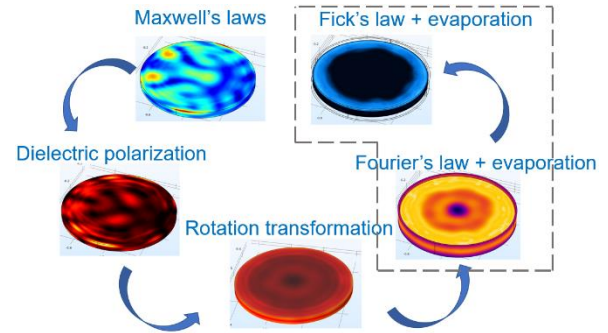


**Figure 1.** Physical sequence of the implemented process.

An in-depth investigation on porous media transport phenomena can be found in literature [8].

### Boundary and initial conditions

The electromagnetic domain is confined by the metallic walls that can be implemented with the condition of perpendicularity of the electric field (Perfect Electric Conductor PEC).

$$\mathbf{n} \times \mathbf{E} = 0 \quad (21)$$

At the input ports, the propagation mode is  $TE_{10}$  [9] and the scattering parameter can be computed:

$$S = \frac{\int_{\partial\Omega} (\mathbf{E} - \mathbf{E}_1) \cdot \mathbf{E}_1 dV}{\int_{\partial\Omega} (\mathbf{E}_1 \cdot \mathbf{E}_1) dV} \quad (22)$$

The heat transfer boundaries are characterized by thermal convection:

$$\mathbf{q} = h(T - T_{ext}) \quad (23)$$

Regarding the moisture transfer boundaries, since the mass depletion term is already included in the governing equation, it is possible to neglect any mass convection as already justified in literature [4]. From absence of moisture transfer can be set at all the boundaries. Initial condition of the electromagnetic model is:

$$\mathbf{E}(x, y, z, 0) = 0 \quad (24)$$

The temperature of the entire model at the beginning of the process is the room temperature

$$T(x, y, z, 0) = T_{room} \quad (25)$$

The initial moisture content is that one of the fresh food product at conservation temperature

$$\theta_l(x, y, z, 0) = \theta_{fresh} \quad (26)$$

## Computational aspects

The imported geometry is presented in Figure 2. The Multiphysics model is characterized by “one-way couplings” and “two-ways coupling”. The electromagnetic step is solved in the frequency domain (the number of simulations is the number of different electric field configurations  $k$  that depends on the specific technology under investigation). The computed results are then imported into the Equation based module to solve the Partial Differential Equations (PDEs) to compute the rotation, and the random selection of electric field patterns. Then the scalar function APD is computed and can be imported into the fully coupled heat transfer and moisture transfer step. The moisture transfer physics has been implemented by using the equation-based module. If the material properties change significantly over the process duration, due to the variation of temperature and moisture, then the electromagnetic step must be computed again, thus closing the loop of computation. A general schema is presented in Figure 3. The used solver is PARDISO (direct solver) and the discretization of the shape functions is of the first order.

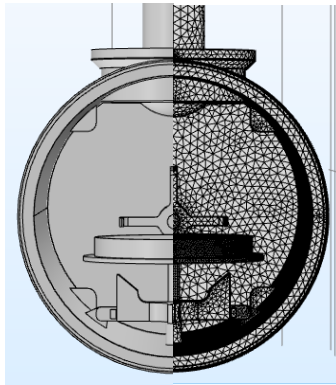


**Figure 2.** Implemented geometry and mesh of the system.

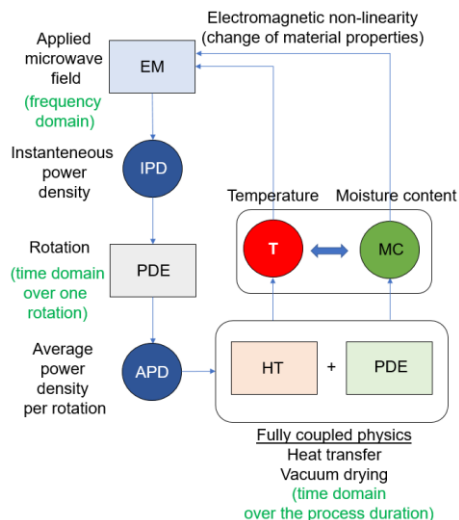


**Figure 3.** Flow chart of the physical coupling between physics and module interfaces.

## Analysis setup

### Main characteristics of the Technology Under Test

The chamber is characterized by a cylindrical shape with main size of 584 mm and 800 mm as diameter and depth respectively. The circular plate is made in PTFE, with an internal diameter of 340 mm, and it is centrally located at the height of 200 mm above the bottom line. The load is formed by apple cubes, forming a uniform layer with 20 mm of thickness. The overall power is 800 W (400 W + 400 W for the two channels system). The analysis is performed over a time domain of 600 s to have small variations of the material properties (as functions of  $\Theta_l, T$ ), and thus assuming the linearity of the complex permittivity. The main geometries and electrical settings that have been used are presented in Figure 4.

### Input parameters

Only the most relevant input parameters of the simulation are here presented:

**Table 1:** Input parameters for simulation purpose.

Parameter	Value [unit]	Source
$f_{rot}$ [Hz]	0.25	-
$D_l$ [ $m^2/min$ ]	1.431e-6	[10]
$k_{vap}$ [1/min]	188.15e-3	[10]
$P_{ch}$ [mBar]	45	-
$\lambda_{wet}$ [W/(m <sup>3</sup> K)]	0.4	[7]
$\lambda_{dry}$ [W/(m <sup>3</sup> K)]	0.12	[7]
$\Delta H$ [kJ/kg]	2460	[6]

## Results

In Figure 5, only one electric field distribution for each technology under test has been presented, but the actual number of computed electric field patterns is  $k$  ( $k = 1$  for the magnetron case,  $k$  is the number of frequencies that have been spanned for the 1-channel SSD system, and  $k = ab$  where  $a$  is the number of frequencies and  $b$  is the number of phase-shifts). The average power density per rotation, and temperature and moisture content after 600 s of processing are depicted.

Regarding the magnetron case, the electric field distribution is highly intense in two regions close to the rim, inducing a higher power transfer rate at the border of the load. A strong cold spot is present in the center, so the drying process is much slower centrally. Also, there is a second annular cold-spot at mid radial position.

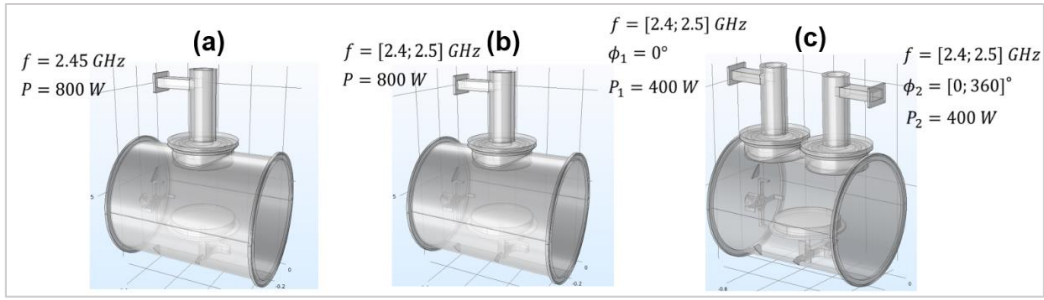


**Figure 4.** General description of the main characteristics of each technology. (a) Magnetron, (b) 1-channel solid-state, (c) 2-channels solid-state.

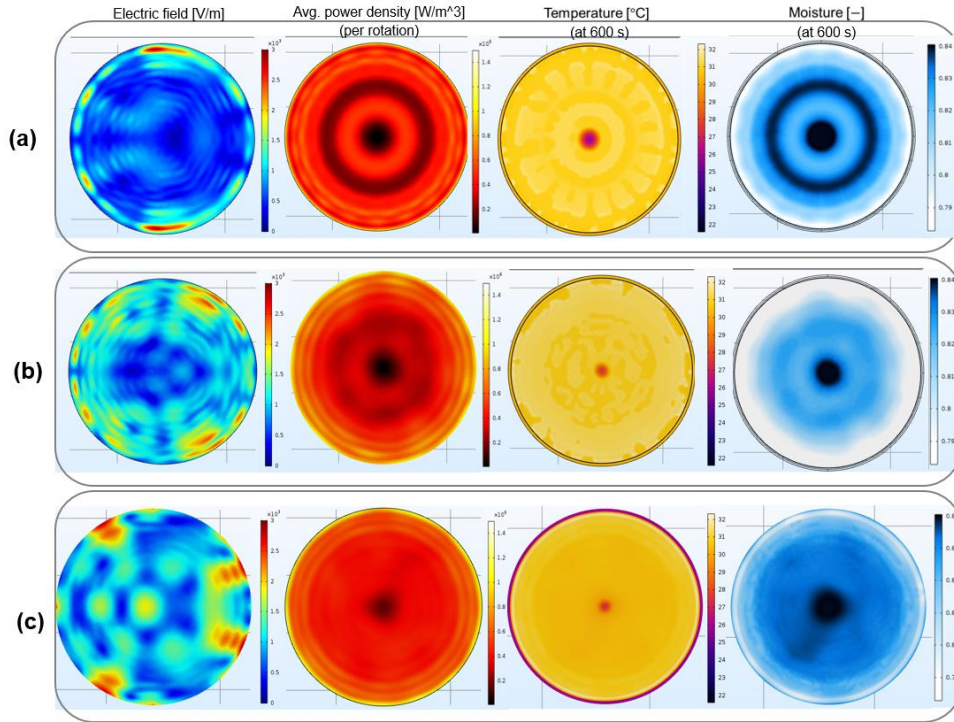


**Figure 5.** Field pattern distributions at a middle height plane (of the load). Electric field magnitude, average power density, temperature and moisture content after 600 s are presented.

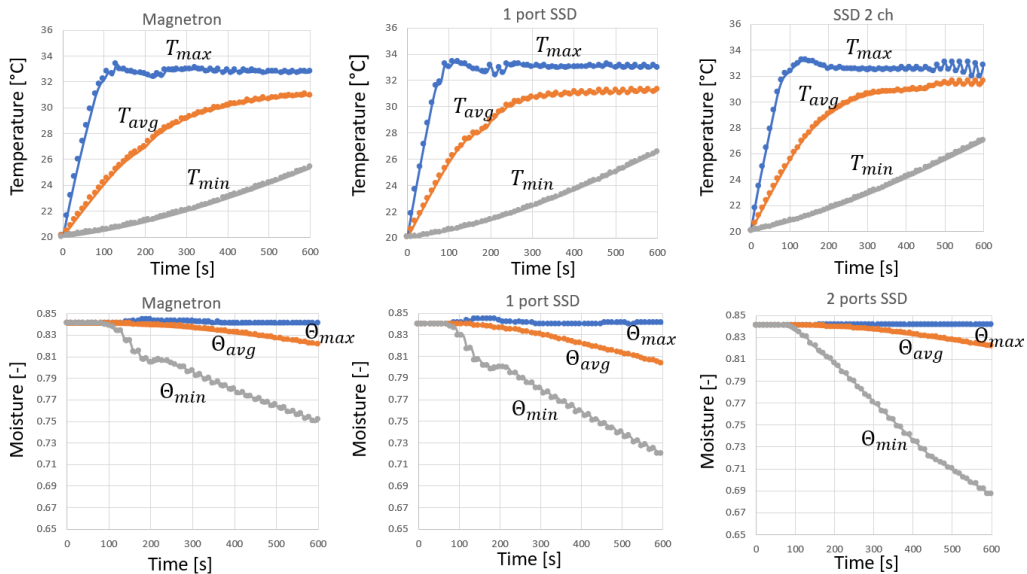


**Figure 6.** The plots show the evolution over time of the temperature and moisture content in terms of minimum, average and maximum in the load volume.

In the case of 1 channel solid state source, the hot-spot is present in a very thin layer close to the rim and the remaining region is more uniformly heated and dried, excepted for the central cold-spot. From the plots in Figure 6, it is possible to note that the 1-channel solid-state system has a higher performance than the classical magnetron system, since the average drying rate increases more over time. On the other hand, the 2-channels solid-state system behaves better than the classical magnetron system, but it requires a proper algorithmic control to perform properly. Indeed, power cross-couplings between the two channels can affect the overall converted power in the load. Despite of lower global performances, the higher potential of the 2-channels solid-state system can be exploited by developing specific algorithms to select complementary field patterns. In Figure 5, it is possible to observe that a hot spot is present in one of the possible configurations, and therefore, selecting this configuration more often than others. Algorithm development can be done using the LiveLink™ for Matlab®.

### Conclusions

From the current analysis, it is verified how a great improvement in terms of heating pattern uniformity can be achieved by using solid-stated technology rather than magnetron technology. The higher the number of the channels and the bigger the number of possible electric field patterns, but cross-coupling can occur, and an average reduction of the converted power is easier. Therefore, for multichannel systems it is important to control the electromagnetic setting in a proper way. Therefore, COMSOL® software is a powerful tool to assess the performances related to different types of microwave technologies, and also, to identify optimal electromagnetic configurations. Further optimization can be performed by creating algorithms in Matlab® and interfacing it with COMSOL® software by using the LiveLink™ for Matlab®.

### Acknowledgments

The authors thank Gigatherm AG for the financial support that has been provided for the current investigation.

### Bibliography

- [1] A. C. Metaxas und R. J. Meredith, *Industrial microwave heating*, IET, 1983.
- [2] A. Wieckowski, P. Korpas, M. Krysicki, F. Dughiero, M. Bullo, F. Bressan und C. Fager, «Efficiency optimization for phase controlled multi-source microwave oven,» *International Journal of Applied Electromagnetics and Mechanics*, pp. 235-241, 2014.
- [3] C. Bianchi, P. Bonato, F. Dughiero und P. Canu, «Enhanced power density uniformity for microwave catalytic reactions adopting solid-state generators: comparison with magnetron technology,» *Chemical Engineering and Processing - Process Intensification*, pp. 286-300, 2017.
- [4] M. Murru, G. Giorgio, S. Montomoli, F. Ricard und F. Stepanek, «Model-based scale-up of vacuum contact drying of pharmaceutical compounds,» *Chemical Engineering Science*, pp. 5045-5054, 2011.
- [5] V. Mykhailyk und N. Lebovka, «Specific heat of apple at different moisture contents and temperatures,» *Journal of Food Engineering*, pp. 32-35, 2014.
- [6] A. Datta, *Biological and Bioenvironmental Heat and Mass Transfer*, Marcel Dekker, Inc., 2002.
- [7] G. Donsi', G. Ferrari and G. Nigro, "Experimental determination of the thermal conductivity of apple and potato at different moisture contents," *Journal of Food Engineering*, pp. 263-268, 1996.
- [8] A. D. Warning, J. M. R. Arquiza und A. K. Datta, «A multiphase porous medium transport model with distributed simulation front to simulate vacuum freezed drying,» *Food Bioproduct Processing*, pp. 637-648, 2015.
- [9] K. Iwabuchi, T. Kubota und T. Kashiwa, «Analysis of Electromagnetic Fields in a Mass-Produced Microwave Oven Using the Finite-Difference Time-Domain Method,» *Journal of Microwave Power and Electromagnetic Energy*, pp. 188-196, 1996.
- [10] C. H. Chong, A. Figiel und C. L. Law, «Combined drying of apple cubes by using of heat pump, vacuum-microwave, and intermittent techniques,» *Food and Bioprocess Technology*, pp. 975-989, 2017.